3D RADAR USING AUGMENTED 2D HARDWARE – SAMPLING AND PROCESSING CONCEPTS

Graeme Jones, Peter Weber, Tim J. Nohara

Accipiter Radar Technologies Inc.

ABSTRACT

This paper explores the means by which 3D radar processing and target tracking can be achieved using conventional 2D marine radar hardware. A typical low-cost marine radar transceiver is coupled with a custom-developed antenna and sophisticated adjunct radar signal/data processor for this task. We look at how a 3D volume may be sampled for a number of different applications, and show how the data can be processed, analysed and visualized as a result. Finally, we provide some example results that have been collected and processed by this radar system.

1. INTRODUCTION

Modern surveillance applications such as homeland security, ground-based sense and avoid (GBSAA) for unmanned aircraft systems (UAS), bird-strike prevention at airports, and radar-activated deterrents and bird monitoring for oil and mining operations can benefit from cost-effective, 3D radar deployments. Even military applications in today's austere environment require more cost-effective solutions. To achieve this, much work has been undertaken over the past decade to exploit inexpensive commercial off-the-shelf (COTS) marine radar hardware with sophisticated, software-definable, radar signal and information processing techniques to significantly improve the performance/price ratio of such systems [1][2].

A novel, 3D surveillance capability that can provide coverage for the entire aerosphere using a two-axis, software-controllable scanner is described in this paper. This enhancement in radar performance is achieved with limited modifications to the hardware and additional sophistication in the software processing to maintain the general low-cost of the system, while adding performance and functionality previously unavailable.

2. DUAL-AXIS SCANNING RADAR

Using a standard COTS marine radar, we have replaced the stock factory antenna (a slotted array antenna) with a custom-designed parabolic reflector antenna. This provides a pencil beam, producing good resolution along both the azimuthal and elevation axes. The usual array antenna only provides a narrow beam in azimuth.

2.1. Elevation Scanner

Replacement of the antenna allows greater accuracy in elevation, but to allow a greater volume swath to be surveyed, beam agility must also be added. This is achieved by use of a servo-controlled motor that can tilt the antenna to any desired elevation angle. The waveguide is also modified to allow the RF energy to still be able to propagate to the antenna dish. Control signals pass through the azimuth rotary joint/slip ring, to and from the elevation servo unit, with the feedback enabling accurate control of the unit's elevation [3]. These additional hardware refinements are performed in-house (as is the control and programming of the elevation scanner), and thus do not significantly increase the cost of the system.

2.2. Implementation

After what is essentially a hardware parts replacement, the dual-axis scanning radar is under full software control. The elevation position is controlled via software while the antenna is performing its usual horizontal scan. Control is achieved by user-definable or dynamic scan tables, which allow the antenna to be steered in elevation, and then to remain at a particular elevation for a variable amount of time. This software control functionality will be explored more in the next section, where we examine 3D sampling and scanning strategies available to the augmented radar system.

3. 3D BEAM-SAMPLING CONCEPTS

3.1. 2D versus 3D

2D scanning radars are well established, and typically employ a wide elevation beam (via the usual slotted array antenna) to capture all activity on the surface and at elevations up to 10 degrees. (For maritime purposes, the wide beam also has the advantage of keeping radiation on the sea surface during the pitching and rolling of the vessel).

If the requirement is to also scan in elevation, then a narrow beam in elevation is required. When a narrower beam is employed, the ability to capture a wide swath of the volume space in any one scan is diminished. As a result, there will be an evitable tradeoff between scan revisit time and total volume scanned.

No 3D radar system (be it mechanically or electronically steered) can scan all of any given volume at once. Target detection and tracking methods are well known for a 2D scanning radar [4], but the problem must be examined more closely when we add the third dimension, or second scanning axis [5].

3.2. Volume Scanning Design

The great advantage of the system described herein is the ability to move the antenna in arbitrary ways in elevation, while still maintaining the usual continuous rotation and scanning in the azimuthal plane. The nature of the design makes it possible to program the elevation scanning pattern to optimize its performance for any given task or function.

An illustration of the dual-axis scanning radar is shown below:

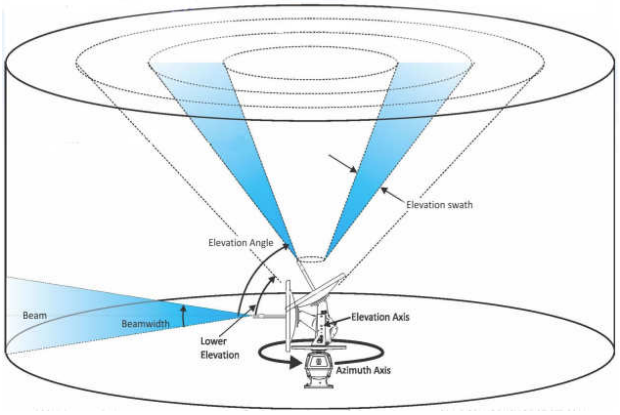

Figure 1 - The dual-axis scanning radar system and associated scan volume

The system shown above has the following characteristics:

DUAL-AXIS SCANNING RADAR SPECIFICATIONS	
Azimuth beamwidth	4 degrees
Elevation beamwidth	4 degrees
Azimuth scanning rate	24 rpm
Maximum elevation scanning rate	1 degree/s

Table 1 - Typical specifications of the dual-axis radar system

The radar is employed in track-while-scan mode, and as such, the rate of detection of a particular target is a critical parameter. If there are too few detections (either from a too long revisit time or a relative speed disproportionate to the scanning rate) then a solid track cannot be established.

The most simple elevation scanning strategy would be to steadily move the beam up and then down between the horizon and zenith to cover the desired volume. From the radar characteristics above, if we desired to sample every possible resolution cell within the volume as quickly as possible, we would have the following results:

FAST SCANNING	
Number of elevation beams	21
Elevation beam stepping interval	4 degrees
Sub-volume dwell time	2.5s
Average scan revisit time	27.5s

Table 2 - Basic volume scanning strategy

This basic, constant-rate scanning strategy has a large revisit time (approaching half a minute), which would be unsuitable for tracking the large majority of airborne targets of interest.

The application of advanced tracking and association algorithms (including multiple-hypothesis and interacting multiple model techniques [6][7]) facilitates the generation high quality tracks can be established with a minimum number of target "hits". As a baseline for this design, we will assume that around 6-12 hits are suitable to acquire a good track state estimate (15-30s). Thus, an alternate design to the fast scanning method above would be to scan each sub-volume (i.e. a particular solid wedge defined by the resolution of the beam) for 15-30 s before moving on. Such a strategy is shown below:

SLOW SCANNING	
Number of elevation beams	21
Elevation beam stepping interval	4 degrees
Sub-volume dwell time	15-30s
Average scan revisit time	157-315s

Table 3 - Slow volume scanning strategy

This would provide enough detections to establish a solid track on any target, with a revisit time of 3-5 minutes. Depending on the mission requirements, this could be a useful volume sampling design.

The main problem with the simple scan tables discussed above is that, for successful target acquisition and tracking, they assume that the target is travelling at a slow enough speed, or moving in a particular way so that it remains in the sub-volume during its scan time. These assumptions may not always be valid, and as a result, more advanced scan patterns may be required to account for more flexible target motion requirements.

3.2.1 Variable elevation rate scanning

Volume scanning via two-dimensional sub-volumes is complicated by the fact that the rate of change of any target's elevation is dependent on both its range from the radar system, as well as its actual velocity. For example, targets at long range will have small elevation rate changes ($\dot{e}_t$), even with relatively high radial velocities, whereas targets at high altitudes and short ranges will have a very high $\dot{e}_t$ even for moderate radial velocities.

As such, to keep a target within a sub-volume, it is required that the radar's scan rate in elevation, $\dot{e}_R$, be close to those of any targets to be acquired under track. The programmable elevation control available in this system makes it possible to design a more sophisticated scanning table that can handle these different elevation rates and thus keep targets of interest within the scanning sub-volume for long enough to acquire a good track.

Let us adopt the concept of a series of scanning bars, which, when combined, create the complete volume scan. The elevation scan rate can differ for each of these bars, as can the range of elevations through which there are scans. The hardest targets to track and acquire are those that will be moving towards or away from the radar, since they will possess the greatest $\dot{e}_t$.

To attempt to capture all required targets, it would be necessary to scan the volume more than once. For example, the slow scanning pattern above provides enough sub-volume dwell to capture targets that are not moving at a greater rate than $\dot{e}_R$, which is of the order of 8°/min there. Targets with an $\dot{e}_t$ much greater than this will simply not be in the scan sub-volume for a long enough time to allow for enough radar hits to establish track. Additional volume scans (which we refer to as bars) are thus necessary to capture these targets and place them under track.

The following table illustrates a more complex scanning scenario, utilizing six bars.

BAR	ELEVATION SPAN (DEG.)	SPEED (DEG/MIN)	SCAN TIME (MIN)
1	6-86	8	10
2	86-20	-24	2.33
3	20-86	40	1.4
4	86-20	-40	1.4
5	20-86	24	2.33
6	86-6	-8	10

Table 4 - Variable rate elevation scanning table

This scan table employs a variable rate elevation scanning. It attempts to take into account targets moving at different $\dot{e}_t$'s, under the assumption that all sub-volumes are equally important.

Examining the table in a little more detail reveals that bars 1 and 6 take into account those targets with a small $\dot{e}_t$ (i.e. those at longer range and low radial velocity), as such targets will remain in the beam on the order of 30s, providing 12 hits and the opportunity to establish a high quality track. Targets at closer range, even with relatively low radial velocities and those faster ones at longer ranges will have an $\dot{e}_t$ potentially much greater than 8°/min, and as such may only be seen by the radar 2 or 3 times in the scan bars. To account for such targets, scan bars 3 and 5 have been created. Similarly, for targets moving at high negative radial velocity, bars 2 and 4 are most useful.

Consider a target moving at an $\dot{e}_t$ of 20 °/min. Based on Table 4, the time it remains in each scan bar is [20 sec, 5 sec, 12 sec, 4 sec, 60 sec, 9 sec]. In this case, bar 5 has provided an opportunity to establish a solid track, on a target that would otherwise have been very difficult to capture with a mechanically scanning antenna. (If the target had an $\dot{e}_t$ of -20 °/min (moving away from the radar), the results would have been [9s, 60s, 4s, 12s, 5s, 20s], which is why the up-down scanning model is used here.)

3.3. Volume Simulation Studies

To further study the volume scanning concepts discussed above, let us consider the following cylindrical scan regions:

Example A: 10km range, 0-1500m height
Example B: 5km range, 0-3000m height

Such scan volumes would be typical for bird monitoring at an environmentally sensitive facility (such as a wind farm, or mine with toxic tailings ponds) or an airport. For these applications, the volume would be considered the general risk region and would need to be monitored 24/7 (although some sub-volumes within the volume may be considered greater risk than others).

To gain some insight into scan coverage and trackability of targets, we will simulate the volumes of interest and populate them with a random number of targets (assumed to be birds for this particular example).

100000 targets are placed at random locations throughout each volume. This of course does not simulate the actual distribution of (bird) targets, but represents an ensemble of possible target locations, trajectories and speeds. Each target is given a random location within the volume, a random ground speed between 10 and 30 m/s (typical for these targets of interest), and a random heading between 0 and 360 degrees. It is assumed that all parameters have

a uniform distribution, and are uncorrelated with one another. The figure below shows the resulting ensemble distribution for example A:

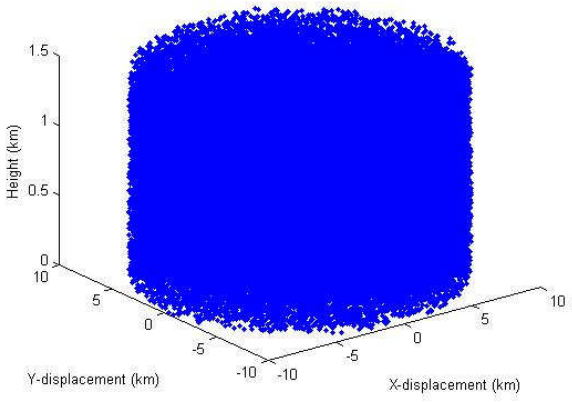

Figure 2 - Distribution of targets within example A's volume space

3.3.1 Target density analysis – Example A

The following table provides a summary of the results for the case of scanning the volume of example A.

BAR #	TRACKABLE TARGETS (%)
1	49.44
2	0.47
3	0.13
4	0.11
5	0.50
6	49.16
Slow Scanning (Table 3)	96.60

Table 5 - Percentage of trackable targets per elevation scan bar

The percentage of trackable targets number displayed in the results table above should be considered an opportunity figure – i.e. the number of hits on the target is adequate to allow for a high quality track to be generated. The results show that, for this particular scan volume, the slow scanning approach (provided in the table for comparison) allows almost all targets to be tracked. In this case, the use of the bars of Table 4 to track targets does not appear to give a particular advantage, although bars 1 and 6 could be used to cover the volume slightly better than slow scanning (only missing an opportunity to track 2% of targets).

Examination of the following figures reveals more details of the above result:

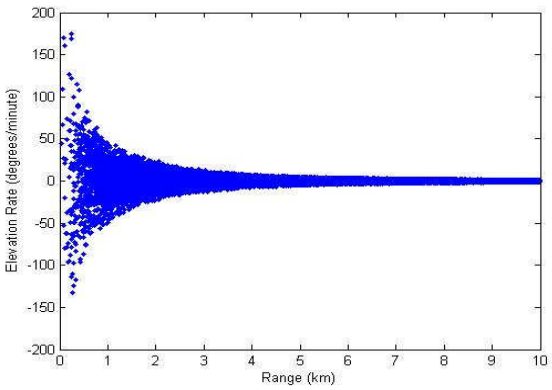

Figure 3 - Scatter plot of elevation rate versus range for target distribution of example A

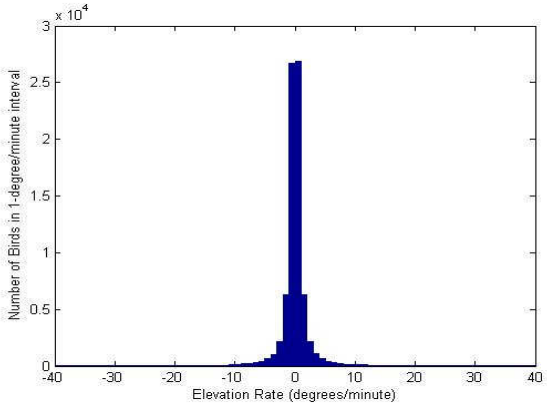

Figure 4 - Histogram of target elevation rate for example A

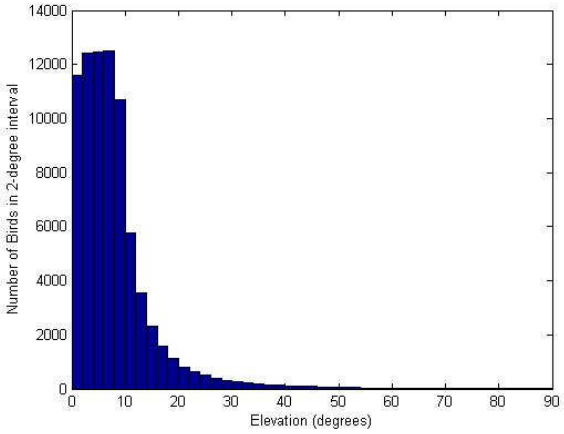

Figure 5 - Histogram of target elevation for example A

Figure 3 shows a scatter plot of elevation rates ($\dot{e}_t$) as a function of range. If the requirement is to scan the whole volume, with no region of designated greater importance, then it is clear that few targets will be missed by not employing the faster elevation rate scanning bars. Indeed the histogram of Figure 4 clearly shows that the large majority of targets fall within the slow scan region of acquisition. For this particular example, slow up-scanning would most likely present an adequate solution, unless

certain volume regions were more important than others. For slightly more coverage, one could utilize bars 1 and 6 of the variable elevation rate scan table. Figure 5 reveals that scan revisit times could be sped up by reducing the highest elevation scanned, since the large majority of targets reside within the first 40° of elevation.

The situation changes, however, if the volume of interest is altered or different emphasis is placed on different regions. If, for example, we reduced the maximum range of interest to 3km, then the slow scanning approach would only detect about 64% of the targets in the space.

3.3.2 Simulated Results – Example B

This second example, which implicitly contains higher altitude, faster $\dot{e}_t$ targets, shows a very different result:

BAR #	TRACKABLE TARGETS (%)
1	46.74
2	2.70
3	0.44
4	0.40
5	2.80
6	46.55
Slow Scanning (Table 3)	78.21

Table 6 - Percentage of trackable targets per elevation scan bar

In this case, the slow scanning fails to adequately provide tracking opportunities over the whole volume. In this case, a minimum of bars 1 and 6 would be required to provide adequate coverage, but it is most likely that bars 2 and 5 would also be required to push the target track opportunities to over 99%.

If we now examine the following scatter plots, we can see why slow scanning is probably inadequate for this volume space.

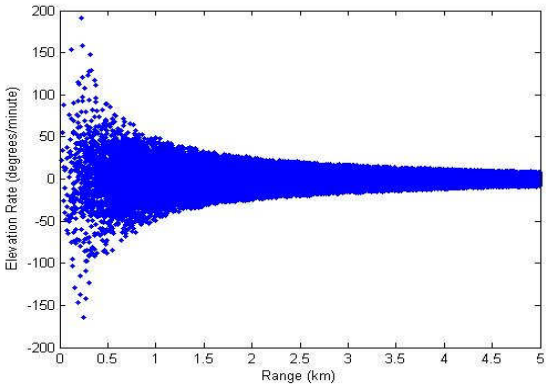

Figure 6 - Scatter plot of elevation rate versus range for target distribution of example B

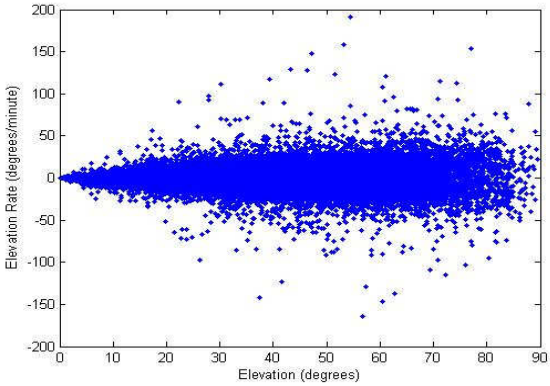

Figure 7 - Scatter plot of elevation rate versus elevation for example B

It is clear that now a greater number of targets can potentially have higher $\dot{e}_t$, and can thus only be acquired for tracking if higher elevation rate scanning is utilized.

The simulation results illustrate the importance of designing a suitable scanning strategy to both cover the required volume and spotlight the designated targets of interest for the mission objectives. This radar system, with its software configurable elevation scanning abilities, allows the scanning bars can be changed at will, and thus can be tailored to the mission-directed volume coverage and target tracking requirements.

3.4. 3D Radar Signal Processing

The radar processing chain is similar to that employed with the unmodified 2D hardware, and details may be found in [1][2][8]. Modifications may sometimes be required, however, due to the differences in the clutter and noise distributions as the radar scans in the vertical plane.

For applications where ground clutter is significant (coupled with a requirement to track and detect targets in the lower elevation regions), the spatial pattern of such clutter will change with a scan elevation change. Under normal 2D scanning operation, the system uses an adaptive clutter map in such cases to suppress the ground clutter. When the antenna steps in elevation, however, the clutter map will be temporarily incorrect, and clutter not masked may create additional false alarms. To mitigate this, the radar processing software can be modified to incorporate a set of dynamically-switchable clutter maps with appropriate clutter map settling times in response to elevation changes.

4. TRACKING WITH THE AUGMENTED 2D RADAR

Due to the nature of the scanning, there is a requirement for robust tracking performance. The tracking system employed here uses multiple hypothesis and interacting

multiple model techniques for association and tracking, via an extended Kalman filter tracking in two-dimensional Cartesian coordinates [1][6][7]. These tracking algorithms have been developed over a number of years; live systems have demonstrated solid tracking performance of more than 1000 tracks, while tolerating PFA's of up to 0.001 [2][8]. This robustness is important, as the volume scan requirement is to acquire a track during the short time that a target is within the sub-volume. The algorithm's tolerance to high PFA's affords better tracking quality within the minimum times we have designed around.

4.1. Slant Range versus Ground Range

Target tracking with 2D scanning radars typically occurs in the slant range plane. The assumption is made that the slant range is commensurate with the ground range, but this can introduce errors in range measurement and subsequently the tracking parameter estimates.

There has been work done at reducing slant range error [9], but here we can go further into the problem by taking into account the altitude estimate itself to assist in converting slant range to ground range. This is important when attempting to fuse tracks from multiple systems, as the registration issues are compounded if there exists a mismatch between ground and slant range.

4.2. Closed-loop tracking and target following

The beam scanning strategies discussed earlier can be thought of as open-loop tracking, in the sense that we are attempting to tailor the beam scan pattern to follow targets displaying certain motion characteristics. A different case would be where we would want to follow a target. For example, it may be desired that a GBSAA radar [10] survey a protective volume surrounding a UAS to ensure that it is operating in an unoccupied airspace. The detection of general aviation aircraft in this dynamic sub-volume would provide awareness to the ground-based pilot to keep the UAS out of harm's way. In a similar manner, aircraft departing an airport could be followed by the radar's dynamic beam to survey a protective sub-volume for the presence of birds.

For such cases, feedback from the tracking system (or a direct external source such as the UAS's own GPS feed) can be employed to effectively steer the radar's beam in a following mode around the aircraft of interest. Here, tracking would necessarily take place in three dimensions, where the altitude estimate can be used to form a 6 state EKF $\begin{pmatrix} x, y, z, \dot{x}, \dot{y}, \dot{z} \end{pmatrix}$. Based on the work undertaken in [11], we could then reformulate the EKF equations by replacing the observation model of equation (3), with

$$z_k = H(x_k) = \begin{pmatrix} r(k) \\ \theta(k) \\ \varphi(k) \end{pmatrix} = \begin{pmatrix} \sqrt{x^2(k)+y^2(k)+z^2(k)} \\ \tan^{-1}\left(\frac{x(k)}{y(k)}\right), \\ \tan^{-1}\left(\frac{z(k)}{\sqrt{x^2(k)+y^2(k)}}\right), \end{pmatrix},$$

to incorporate the elevation measure ϕ (with Z_k as the k^{th} measurement vector and X_k the corresponding state). The linearized Jacobian observation matrix of equation (4) in [11] could then be re-expressed as:

$$H_k^i = \left.\frac{\partial H(x)}{\partial x}\right|_{\hat{x}_{k|k-1}}$$

$$= \begin{pmatrix} \frac{y}{\sqrt{x^2+y^2+z^2}} & \frac{y}{\sqrt{x^2+y^2+z^2}} & \frac{y}{\sqrt{x^2+y^2+z^2}} & 0 & 0 & 0 \\ \frac{y}{x^2+y^2} & \frac{-x}{x^2+y^2} & 0 & 0 & 0 & 0 \\ \frac{-xz}{(x^2+y^2+z^2)\sqrt{x^2+y^2}} & \frac{-yz}{(x^2+y^2+z^2)\sqrt{x^2+y^2}} & \frac{\sqrt{x^2+y^2}}{(x^2+y^2+z^2)} & 0 & 0 & 0 \end{pmatrix}_{\hat{x}_{k|k-1}}$$

5. RCS PROFILE ESTIMATION

Radar cross section (RCS) is very useful for classification of target types. In bird-strike prevention and GBSAA applications, RCS of birds can also be used in the measuring of risk of collision with aircraft. RCS estimation can be performed in real-time to provide target size estimates. RCS profiling, which generates an RCS picture of a target, is a much more difficult task and is typically done off-line. The process by which these profiles can be generated is based upon the high quality tracking available via the radar systems discussed here, combined with sophisticated post-processing. With the advantage of altitude estimation, more accurate RCS profiles can be generated, due to the improved height estimations available.

The procedure involves extracting a track (or collection of tracks) belonging to a target of interest. With the state estimate available via the filtered track output, the heading of the target on track can be estimated. These estimates are then used to determine the target aspect that is being observed at the time. The RCS estimate, which is coupled with the track, is then used to build up a polar plot of the profile, depending on the aspect of the target. If the target is tracked often enough, the data will accumulate to allow a more complete diagram of the RCS profile (versus aspect) to be constructed [12]. Use of the additional elevation dimension allows a further refinement of the results.

The figures below show a preliminary example of creating an RCS profile for an ultralight aircraft under track. The data was obtained using the radar system described herein. Figure 8 shows the azimuthal profile generated based on reconstruction using the heading

information available via the track state. The next view (Figure 9) displays a projection of the 3D RCS profile, which is possible via the addition of elevation information. The RCS information in three dimensions is projected into the X-Z plane for the plot, which would have the nose of the aircraft coming out of the page. (These RCS profiles are derived from the ultralight aircraft tracked in Figure 12).

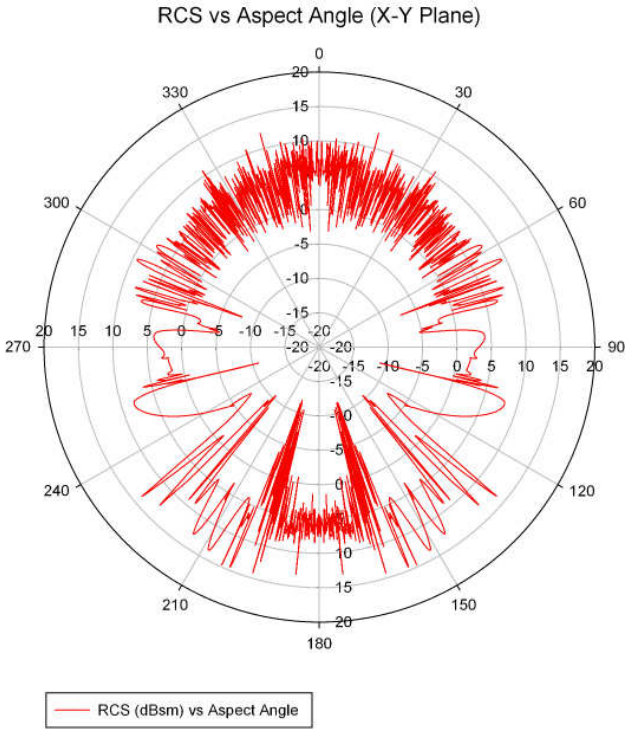

Figure 8 - RCS planar profile

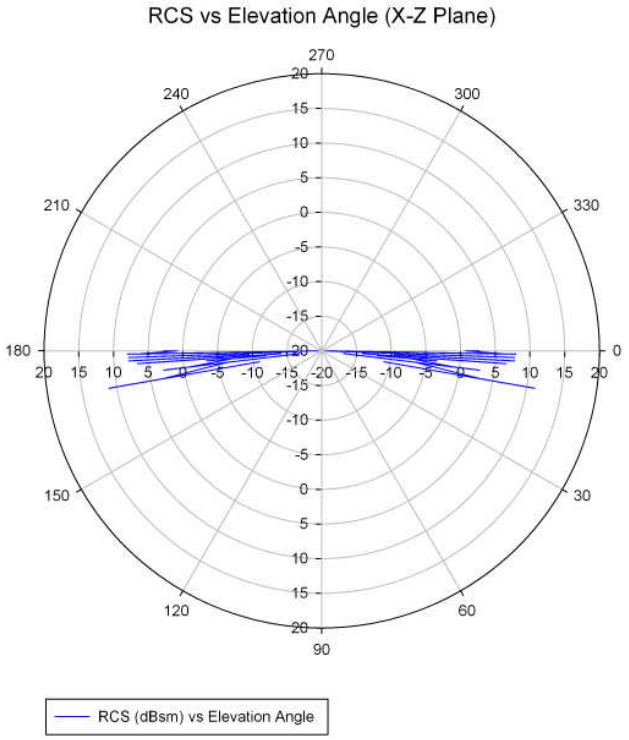

Figure 9 - RCS head-on projected profile

6. REAL DATA RESULTS

The following figures show a variety of tracks obtained via the dual-axis scanning system, deployed at two different locations, one where birds were tracked and the second where an ultralight aircraft was tracked.

Figure 10 - Planar view of bird tracks

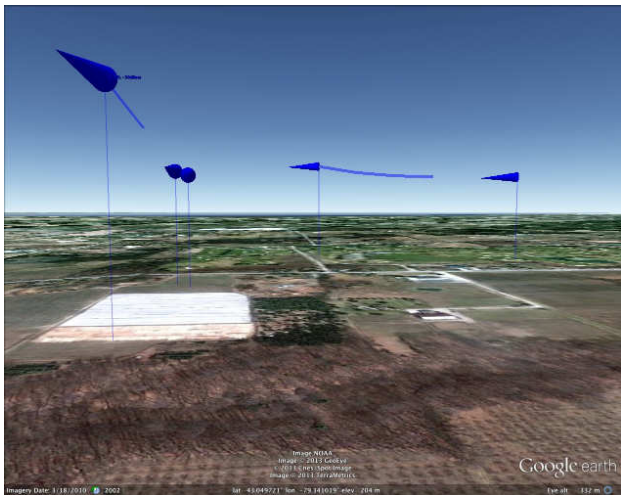

Figure 11 - Titled view of bird tracks showing altitude

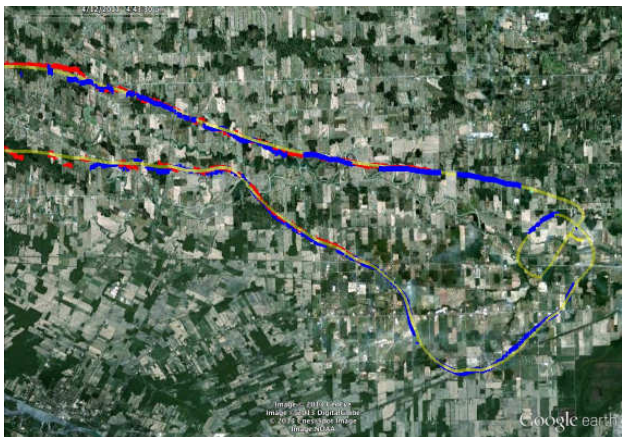

Figure 12 - Planar view of ultralight aircraft tracked with fixed (red) and dual-axis (blue) radar systems

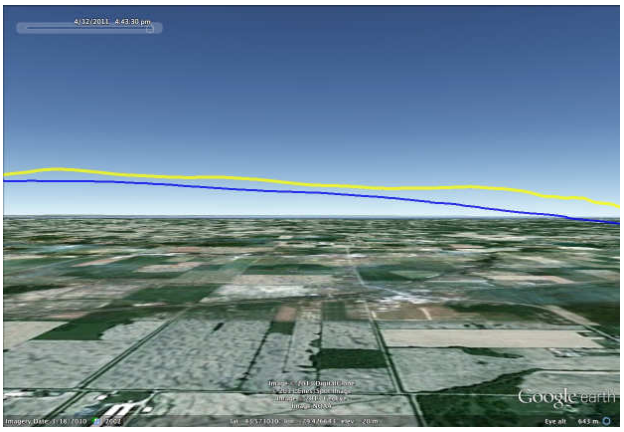

Figure 13 - Close-up of GPS log and corresponding dual-axis scanner track of ultralight aircraft

Figure 10 above shows a snapshot of a live display of birds being tracked by the system. The tilted view of Figure 11 provides a better view of the actual track states, complemented with altitude information.

The final two figures show the results of tracking an ultralight aircraft as it flies a loop pattern. Figure 12 shows a comparison between the tracks produced by a fixed elevation antenna (shown in red) and the dual-axis scanner (blue). The dual-axis system used a variable rate elevation scan similar to the one shown in Table 4 over the desired volume of interest. For comparison, the actual GPS log of the flight is shown in yellow. It may be seen from Figure 12 that the variable elevation scan pattern has produced greater track coverage than the fixed antenna. This underlines the advantage of using the 3D system supported by a customized scan pattern for the required mission. A close-up view of a section of the track (Figure 13) shows a close correspondence with the reported aircraft position (yellow) via the GPS logger.

7. SUMMARY

We have presented here an introduction to affordable 3D coverage and surveillance of the aerosphere by exploiting low-cost, high-resolution COTS 2D X-band marine radars, coupled with an antenna modification and sophisticated radar signal processing. The challenge is to be able to efficiently scan the 3D cylindrical or spherical volume of interest for the particular mission or application and extract useful target information. 3D scanning and volume sampling requirements have been discussed for a few modern applications, and some novel software-definable scan design strategies have been examined. Examples of 3D target trajectory generation (tracking) and RCS profiling that can be obtained with suitably matched radar signal and data processing are also provided. These excellent results motivate future efforts to deploy and optimize solutions for particular applications, based on specific mission requirements. Suitably measuring 3D RCS profiles for targets of interest, building target libraries, and developing automated target matching/recognition algorithms is the subject of future R&D.

8. ACKNOWLEDGEMENTS

The authors would like to than Sean Clifford for his assistance in producing the figures, and for his valuable comments and suggestions.

9. REFERENCES

[1] T.J. Nohara, "A commercial approach to successful persistent radar surveillance of sea, air and land along the northern border," 2010 IEEE International Conference on Technologies for Homeland Security, 8-10 November 2010, Waltham, MA.

[2] T.J. Nohara, A. Premji, A. Ukrainec, P. Weber, G. Jones and C. Krasnor, "Low-cost, high-performance radar networks", US Patent No. 7940206 B2, May 10, 2011.

[3] P. Weber and T.J Nohara, "Device and method for 3D height-finding radar", US Patent No. 7864103 B2, Jan 4, 2011.

[4] Y. Bar-Shalom and T.E. Fortmann, *Tracking and Data Association*, Academic Press, 1988.

[5] T.J. Nohara, P. Weber, A. Ukrainec, A. Premji, G. Jones, N. Costa, R. Beason, "Device and method for 3D sampling with avian radar", US Patent App. No. 61/532812, Sep 9, 2011.

[6] D. Reid, "An algorithm for tracking multiple targets", *IEEE Trans. Automatic Control*, vol. 24, issue 6, pp. 843-854, Dec. 1979.

[7] G. Watson and D. Blair, "An algorithm for tracking targets that maneuver through coordinated turns," *Proc. SPIE,* vol. 1698, pp. 236-247,Apr. 20-22, 1992.

[8] T.J. Nohara, P. Weber, A. Premji, C. Krasnor, S. Gauthreaux, M. Brand and G. Key, "Affordable avian radar surveillance systems for natural resource management and BASH applications", in *Proc. IEEE Int. Radar Conf.*, pp 10-15, 2005.

[9] E. H. Aoki, "A general approach for altitude estimation and mitigation of slant range errors on target tracking using 2D radars", *Proc. 13th Int. Conf. on Information Fusion (FUSION)*, Edinburgh, UK, pp 1-8, Jul 2010.

[10] M. Wilson, "The Use of Low-Cost Mobile Radar Systems for Small UAS Sense and Avoid", Chapter 11 in *Sense and Avoid in UAS: Research and Applications*, P. Angelov ed., Wiley, 2012.

[11] G. Ming-Jiu, Y. Xiao, H. You, S. Bao, "An approach to tracking a 3-D target with 2-D radar," in *Proc. IEEE Int. Radar Conference,* Arlington, VA, pp. 11-14, May 2005.

[12] G. Jones and T.J. Nohara, "Wide area radar networks with data persistence", *Proc. 11th Int. Conf. on Int. Sc., Sig. Proc. and their App. (ISSPA)*, Montreal, QC, pp 1159-1164, July 2012.